Review of p-y relationships in cohesionless soil

Brødbæk, K. T.; Møller, M.; Sørensen, S. P. H.; Augustesen, Anders Hust

Publication date:
2009

Document Version
Publisher's PDF, also known as Version of record

Review of *p-y* relationships in cohesionless soil

K.T. Brødbæk
M. Møller
S.P.H. Sørensen
A.H. Augustesen

ISSN 1901-726X
DCE Technical Report No. 57

AALBORG UNIVERSITY
Department of Civil Engineering

Aalborg University
Department of Civil Engineering
Water & Soil

DCE Technical Report No. 57

Review of *p-y* relationships in cohesionless soil

by

K.T. Brødbæk
M. Møller
S.P.H. Sørensen
A.H. Augustesen

January 2009

Scientific Publications at the Department of Civil Engineering

Technical Reports are published for timely dissemination of research results and scientific work carried out at the Department of Civil Engineering (DCE) at Aalborg University. This medium allows publication of more detailed explanations and results than typically allowed in scientific journals.

Technical Memoranda are produced to enable the preliminary dissemination of scientific work by the personnel of the DCE where such release is deemed to be appropriate. Documents of this kind may be incomplete or temporary versions of papers—or part of continuing work. This should be kept in mind when references are given to publications of this kind.

Contract Reports are produced to report scientific work carried out under contract. Publications of this kind contain confidential matter and are reserved for the sponsors and the DCE. Therefore, Contract Reports are generally not available for public circulation.

Lecture Notes contain material produced by the lecturers at the DCE for educational purposes. This may be scientific notes, lecture books, example problems or manuals for laboratory work, or computer programs developed at the DCE.

Theses are monograms or collections of papers published to report the scientific work carried out at the DCE to obtain a degree as either PhD or Doctor of Technology. The thesis is publicly available after the defence of the degree.

Latest News is published to enable rapid communication of information about scientific work carried out at the DCE. This includes the status of research projects, developments in the laboratories, information about collaborative work and recent research results.

Published 2009 by
Aalborg University
Department of Civil Engineering
Sohngaardsholmsvej 57,
DK-9000 Aalborg, Denmark

Printed in Aalborg at Aalborg University

ISSN 1901-726X
DCE Technical Report No. 57

Review of p–y relationships in cohesionless soil

K. T. Brødbæk[1]; M. Møller[2]; S. P. H. Sørensen[3]; and A. H. Augustesen[4]

Aalborg University, January 2009

Abstract

Monopiles are an often used foundation concept for offshore wind turbine converters. These piles are highly subjected to lateral loads and thereby bending moments due to wind and wave forces. To ensure enough stiffness of the foundation and an acceptable pile-head deflection, monopiles with diameters at 4 to 6 m are typically necessary. In current practice these piles are normally designed by use of the p–y curve method although the method is developed and verified for small diameter, slender piles with a diameter up to approximately 2 m. In the present paper a review of existing p–y curve formulations for piles in sand under static loading is presented. Based on numerical and experimental studies presented in the literature, advances and limitations of current p–y curve formulations are outlined.

1 Introduction

It is a predominating opinion that the global warming is caused by the emission of greenhouse gasses. According to United Nations (1998) there is a strong political interest to raise the percentage of renewable energy, and reduce the use of fossil fuels, in the years to come. Wind energy plays a major role in attaining these goals both onshore and offshore which is why a further development is of interest.

Several concepts for offshore wind turbine foundations exist. The choice of foundation concept primarily depends on site conditions and the dominant type of loading. At great water depths the most common foundation principle is monopiles, which are single steel pipe piles. The foundation should be designed to have enough ultimate resistance against vertical and lateral loads. Moreover, the deformation criteria and stiffness of the foundations should be acceptable under lateral loading which is normally the primary design criterion for this type of foundation. In order to avoid resonance the first natural frequency of the structure needs to be between $1P$ and $3P$, where P denotes the frequency corresponding to one rotor rotation. According to LeBlanc et al. (2007) monopiles installed recently have diameters around 4 to 6 m and a pile slenderness ratio (L/D) around 5 where L is the embedded length and D is the outer pile diameter.

In current design of laterally loaded offshore monopiles, p–y curves are normally used. A p–y curve describes the nonlinear relationship between the soil resistance acting against the pile wall, p, and

[1]Graduate Student, Dept. of Civil Engineering, Aalborg University, Sohngaardsholmsvej 57, 9000 Aalborg, Denmark.

[2]Graduate Student, Dept. of Civil Engineering, Aalborg University, Sohngaardsholmsvej 57, 9000 Aalborg, Denmark.

[3]Graduate Student, Dept. of Civil Engineering, Aalborg University, Sohngaardsholmsvej 57, 9000 Aalborg, Denmark.

[4]Assistant Professor, Dept. of Civil Engineering, Aalborg University, Sohngaardsholmsvej 57, 9000 Aalborg, Denmark.

the lateral deflection of the pile, y. Note that there in present paper is distinguished between soil resistance, p, and ultimate soil resistance, p_u. The soil resistance is given as the reaction force per unit length acting on the pile until reaching the ultimate soil resistance. The ultimate soil resistance is given as the point of maximum soil resistance.

Several formulations of p–y curves exist depending on the type of soil. These formulations are originally formulated to be employed in the offshore gas and oil sector. However they are also used for offshore wind turbine foundations, although piles with significantly larger diameter and significantly smaller slenderness ratio are employed for this type of foundation.

In this paper the formulation and implementation of p–y curves proposed by Reese et al. (1974) and API (1993) for piles in sands due to static loading will be analysed. However, alternative methods for designing laterally loaded piles have been proposed in the literature. According to Fan and Long (2005) these alternative approaches can generally be classified as follows:

- The limit state method.
- The subgrade reaction method.
- The elasticity method.
- The finite element method.

Simplest of all the methods are the limit state methods, e.g. Broms (1964), considering only the ultimate soil resistance.

The simplest method for predicting the soil resistance due to a given applied horizontal deflection is the subgrade reaction method, e.g. Reese and Matlock (1956) and Matlock and Reese (1960). In this case the soil resistance is assumed linearly dependent on the pile deflection. Full-scale tests though substantiate a non-linear relationship between soil resistance and pile deflection. The subgrade reaction method must therefore be considered too simple and highly inaccurate. In addition the subgrade reaction method is not able to predict the ultimate lateral resistance. The p–y curve method assumes a non-linear dependency between soil resistance and pile deflection and is therefore able to produce a more accurate solution. Furthermore the ultimate lateral resistance can be estimated by using the p–y curve method.

In both the p–y curve method and the subgrade reaction method the winkler approach, cf. section 2, is employed to calculate the lateral deflection of the pile and internal forces in the pile. When employing the Winkler approach the pile is considered as a beam on an elastic foundation. The beam is supported by a number of uncoupled springs with spring stiffness given by p–y curves. When using the Winkler approach the soil continuity is not taken into account as the springs are considered uncoupled.

The elasticity method, e.g. Banerjee and Davis (1978), Poulos (1971), and Poulos and Davis (1980), includes the soil continuity. However, the response is assumed to be elastic. As soil is more likely to behave elasto-plastically, this elasticity method is not to be preferred unless only small strains are considered. Hence, the method is only valid for small strains and thereby not valid for calculating the ultimate lateral resistance.

Another way to deal with the soil continuity and the non-linear behaviour is to apply a three-dimensional finite element model, e.g. Abdel-Rahman and Achmus (2005). When applying a three-dimensional finite element model both deformations and the ultimate lateral resistance can be calculated. Due to the complexity of a three-dimensional model,

substantial computational power is needed and calculations are often very time consuming. Phenomena such as liquifaction, due to non-appropriate kinematic models, and gaps between soil and pile are at present hard to handle in the models. Hence, a finite element approach is a useful method but the accuracy of the results is highly dependent on the applied constitutive soil models as well as the calibration of these models.

2 p–y curves and Winkler approach

As a consequence of the oil and gas industry's expansion in offshore platforms in the 1950s, models for design of laterally loaded piles were required. The key problem is the soil-structure interaction as the stiffness parameters of the pile, E_p, and the soil, E_s, may be well known but at the soil-pile interface the combined parameter E_{py} is governing and unknown. In order to investigate this soil-pile interaction a number of full-scale tests on fully instrumented piles have been conducted and various expressions depending on the soil conditions have been derived to predict the soil pressure on a pile subjected to lateral loading.

Historically, the derivation of the p–y curve method for piles in sand is as follows:

- Analysing the response of beams on an elastic foundation. The soil is characterised by a series of linear-elastic uncoupled springs, introduced by Winkler (1867).
- Hetenyi (1946) presents a solution to the beam on elastic foundation problem.
- McClelland and Focht (1958) as well as Reese and Matlock (1956) suggest the basic principles in the p–y curve method.
- Investigations by Matlock (1970) indicates that the soil resistance in one point is independent of the pile deformation above and below that exact point.
- Tests on fully instrumented test piles in sand installed at Mustang Island are carried out in 1966 and reported by Cox et al. (1974).
- A semi-empirical p–y curve expression is derived based on the Mustang Island tests, cf. Reese et al. (1974). The expression becomes the state-of-the-art in the following years.
- Murchison and O'Neill (1984) compare the p–y curve formulation proposed by Reese et al. (1974) with three simplified expressions (also based on the Mustang Island tests) by testing the formulations against a database of relatively well-documented lateral pile load tests. A hyperbolic form is found to provide better results compared to the original expressions formulated by Reese et al. (1974).

Research has been concentrated on deriving empirical (e.g. Reese et al. 1974) and analytical (e.g. Ashour et al. 1998) p–y curve formulations for different types of soil giving the soil resistance, p, as a function of pile displacement, y, at a given point along the pile. The soil pressure at a given depth, x_t, before and during a static excitation is sketched in fig. 1b. The passive pressure on the front of the pile is increased as the pile is deflected a distance y_t while the active pressure at the back is decreased.

An example of a typical p–y curve is shown in fig 2a. The curve has an upper horizontal limit denoted by the ultimate soil resistance, p_u. The horizontal line implies that the soil behaves plastically meaning that

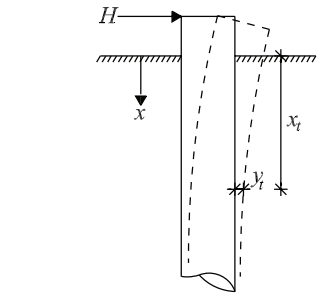

(a) Pile bending due to lateral loading.

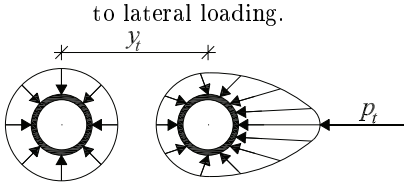

(b) Stresses on a pile before and during lateral excitation.

Figure 1: Distribution of stresses before and during lateral excitation of a circular pile. p_t denotes the net force acting on the pile at the depth x_t, after Reese and Van Impe (2001).

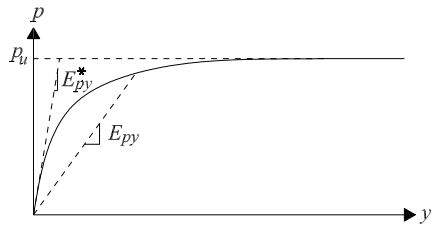

(a) p–y curve.

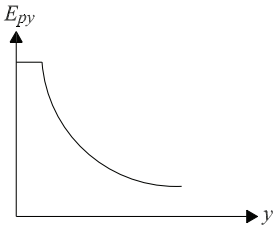

(b) Variation of subgrade reaction modulus.

Figure 2: Typical p–y curve and variation of the modulus of subgrade reaction at a given point along the pile, after Reese and Van Impe (2001).

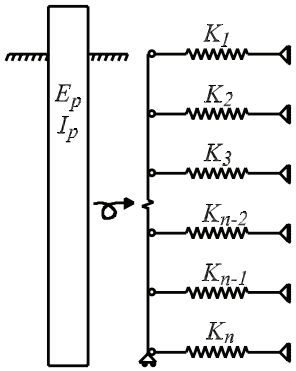

Figure 3: The Winkler approach with the pile modelled as an elastic beam element supported by non-linear uncoupled springs. K is the stiffness corresponding to E_{py}.

no loss of shear strength occurs for increasing strain. The subgrade reaction modulus, E_{py}, at a given depth, x, is defined as the secant modulus p/y. E_{py} is thereby a function of both lateral pile deflection, y, and depth, x, as well as the physical properties and load conditions. E_{py} does not uniquely represent a soil property, but is simply a convenient parameter that describes the soil-pile interaction. E_{py} is constant for small deflections for a particular depth, but decreases with increased deflection, cf. fig. 2b. A further examination of the shape of p–y curves is to be found in section 3, and an overview of the used parameters are given in tab. 1.

Since the pile deflection is non-linear a convenient way to obtain the soil resistance along the pile is to apply the Winkler approach where the soil resistance is modelled as uncoupled non-linear springs with stiffness K_i acting on an elastic beam as shown in fig. 3. K_i is a non-linear load transfer function corresponding to E_{py}. By employing uncoupled springs layered soils can conveniently be modelled.

The governing equation for beam deflection was stated by Timoshenko (1941). The equation for an infinitesimal small element, dx, located at depth x, subjected to lateral loading, can be derived from static equilibrium. The sign convention in fig. 4 is employed. N, V, and M defines the axial force, shear force and bending moment, respectively. The axial force, N, is assumed to act in the cross-section's centre of gravity.

Equilibrium of moments and differentiating with respect to x leads to the following equation where second order terms are

Table 1: Definition of parameters and dimensions used in the present paper.

Description	Symbol	Definition	Dimension
Pile diameter	D		L
Pile length	L		L
Soil resistance	p		F/L
Ultimate resistance	p_u		F/L
Soil pressure	P	$P = p/D$	F/L^2
Pile deflection	y		L
Depth below soil surface	x		L
Second moment of inertia	I_p		L^4
Young's modulus of elasticity of the pile	E_p		F/L^2
Modulus of subgrade reaction	E_{py}	$E_{py} = p/y$	F/L^2
Initial stiffness	E^*_{py}	$E^*_{py} = \frac{dp}{dy}$, $y = 0$	F/L^2
Initial modulus of subgrade reaction	k		F/L^3

neglected:

$$\frac{d^2M}{dx^2} + \frac{dV}{dx} - N\frac{d^2y}{dx^2} = 0 \qquad (1)$$

Following relations are used:

$$M = E_pI_p\kappa \qquad (2)$$

$$\frac{dV}{dx} = -p \qquad (3)$$

$$p(y) = -E_{py}y \qquad (4)$$

E_p and I_p are the Young's modulus of elasticity of the pile and the second moment of inertia of the pile, respectively. κ is the curvature strain of the beam element.

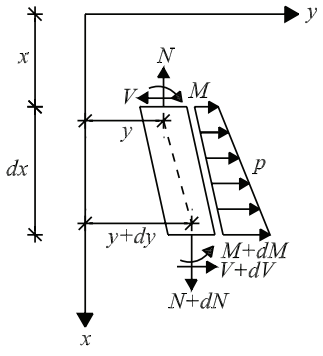

Figure 4: Sign convention for infinitesimal beam element.

Use of (2)–(4) and the kinematic assumption $\kappa = \frac{d^2y}{dx^2}$ which is valid in Bernoulli-Euler beam theory the governing fourth-order differential equation for determination of deflection is obtained:

$$E_pI_p\frac{d^4y}{dx^4} - N\frac{d^2y}{dx^2} + E_{py}y = 0 \qquad (5)$$

In (5) the shear strain, γ, in the beam is neglected. This assumption is only valid for relatively slender beams. For short and rigid beams the Timoshenko beam theory, that takes the shear strain into account, is preferable. The following relations are used:

$$V = G_pA_v\gamma \qquad (6)$$

$$\gamma = \frac{dy}{dx} - \omega \qquad (7)$$

$$\kappa = \frac{d\omega}{dx} \qquad (8)$$

G_p and A_v are the shear modulus and the effective shear area of the beam, respectively. ω is the cross-sectional rotation defined in fig. 5. In Timoshenko beam theory the shear strain and hereby the shear stress is assumed to be constant over the cross section. However, in reality the shear stress varies parabolic over the cross section. The effective shear area is defined so the two stress variations give the same shear force. For a pipe the effective shear area can be calculated as:

$$A_v = 2(D - t)t \qquad (9)$$

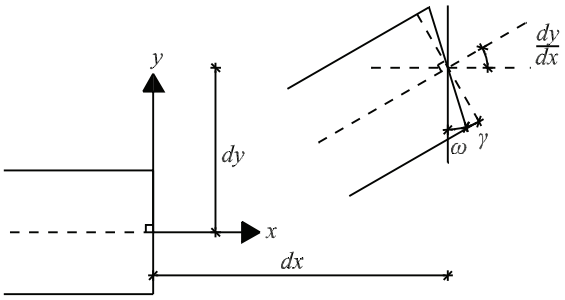

Figure 5: Shear and curvature deformation of a beam element.

where t is the wall thickness of the pipe.

By combining (1) – (4) and (6) – (8) two coupled differential equations can be formulated to describe the deflection of a beam:

$$GA_v \frac{d}{dx}\left(\frac{dy}{dx} - \omega\right) - E_{py} y = 0 \qquad (10)$$

$$E_p I_p \frac{d^3\omega}{dx^3} - N\frac{d^2y}{dx^2} + E_{py} y = 0 \qquad (11)$$

In the derivation of the differential equations the following assumptions have been used:

- The beam is straight and has a uniform cross section.
- The beam has a longitudinal plane of symmetry, in which loads and reactions lie.
- The beam material is homogeneous, isotopic, and elastic. Furthermore, plastic hinges do not occur in the beam.
- Young's modulus of the beam material is similar in tension and compression.
- Beam deflections are small.
- The beam is not subjected to dynamic loading.

3 Formulations of p–y curves for sand

p–y curves describing the static behaviour of piles in cohesionless soils are described followed by a discussion of their validity and limitations. Only the formulation made by Reese et al. (1974), hereafter denoted Method A, and the formulation proposed by API (1993), Method B, will be described. Both p–y curve formulations are empirically derived based on full-scale tests on free ended piles at Mustang Island.

3.1 Full-scale tests at Mustang Island

Tests on two fully instrumented, identical piles located at Mustang Island, Texas as described by Cox et al. (1974), are the starting point for the formulation of p–y curves for piles in sand. The test set up is shown in fig. 6.

To install the test- and reaction piles a Delmag-12 diesel hammer was used. The test piles were steel pipe piles with a diameter of 0.61 m (24 in) and a wall thickness of 9.5 mm (3/8 in). The embedded length of the piles was 21.0 m (69 ft) which corresponds to a slenderness ratio of $L/D = 34.4$. The piles were instrumented with a total of 34 active strain gauges from 0.3 m above the mudline to 9.5 m (32 ft) below the mudline. The strain gauges were bonded directly to the inside of the pile in 17 levels with highest concentration of gauges near the mudline. The horizontal distance between the centre of the two test piles was 7.5 m (24 ft and 8 in). Between the piles the load cell was installed on four reaction piles. The minimum horizontal distance from the centre of a reaction pile to the centre of a test pile was 2.8 m (9 ft and 4 in). The water table was located at the soil surface, hereby the soil was fully saturated.

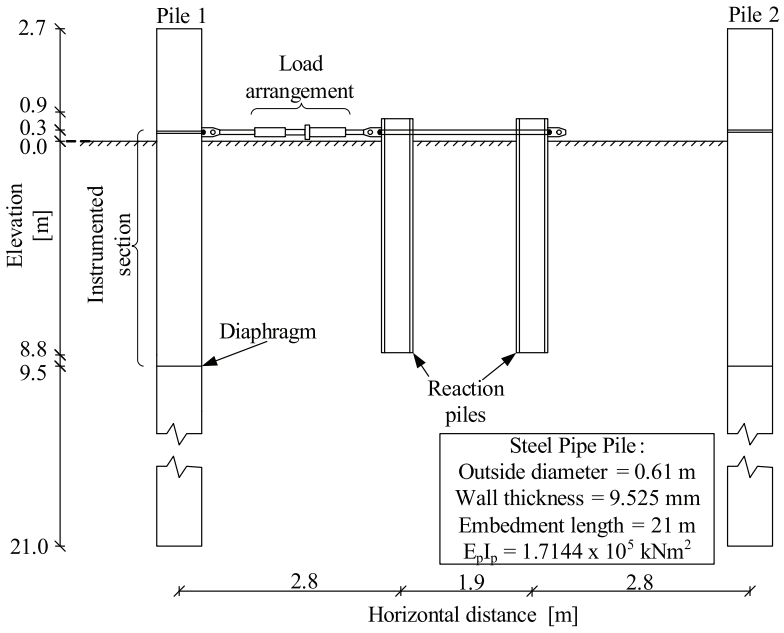

Figure 6: Set-up for Mustang Island tests, after Cox et al. (1974).

Prior to pile installation, two soil borings were made, each in a range of 3.0 m (10 ft) from a test pile. The soil samples showed a slight difference between the two areas where the piles were installed, as one boring contained fine sand in the top 12 m and the other contained silty fine sand. The strength parameters were derived from standard penetration tests according to Peck et al. (1953). The standard penetration tests showed large variations in the number of blows per ft. Especially in the top 40 ft of both borings the number of blows per ft varied from 10 to 80. From 40 to 50 ft beneath the mudline clay was encountered. Beneath the clay layer the strength increased from 40 to 110 blows per ft. From 60 ft beneath the mudline to the total depth the number of blows per ft decreased from 110 to 15.

The piles were in total subjected to seven horizontal load cases consisting of two static and five cyclic. Pile 1 was at first subjected to a static load test 16 days after installation. The load was applied in steps until a maximum load of 267 kN (60000 lb) was reached. The maximum load was determined as no failure occurred in the pile. After the static load test on pile 1 two cyclic load tests were conducted. 52 days after installation a pull-out test was conducted on pile 2. A maximum of 1780 kN (400000 lb) was applied causing the pile to move 25 mm (1 inch). After another week pile 2 was subjected to three cases of cyclic loading and finally a static load test. The static load case on pile 2 was performed immediately after the third cyclic load case which might affect the results. Reese et al. (1974) do not clarify whether this effect is considered in the analyses.

3.2 Method A

Method A is the original method based on the Mustang Island tests, cf. Reese et al. (1974). The p–y curve formulation consists of three curves: an initial straight line, p_1, a parabola, p_2, and a straight line, p_3, all assembled to one continuous piecewise differentiable curve, cf. fig. 7. The last straight line from (y_m,p_m) to (y_u,p_u) is bounded by an upper limit characterised by the ultimate resistance, p_u.

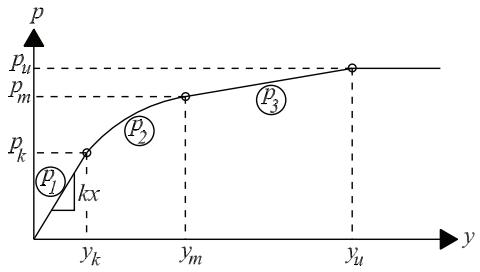

Figure 7: p–y curve for static loading using method A, after Reese et al. (1974).

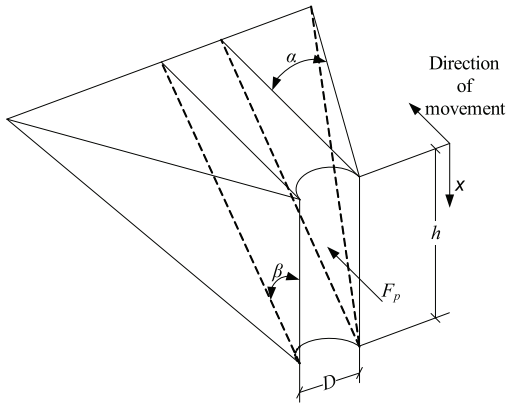

Figure 8: Failure mode for shallow depths, after Reese et al. (1974).

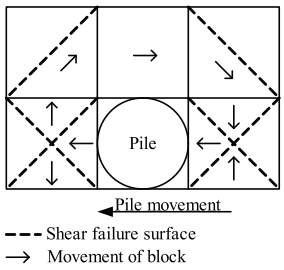

Figure 9: Failure mode for deep depths, after Reese et al. (1974).

Ultimate resistance

The total ultimate lateral resistance, F_{pt}, is equal to the passive force, F_p, minus the active force, F_a, on the pile. The ultimate resistance can be estimated analytically by means of either statically or kinematically admissible failure modes. At shallow depths a wedge will form in front of the pile assuming that the Mohr-Coulomb failure theory is valid. Reese et al. (1974) uses the wedge shown in fig. 8 to analytically calculate the passive ultimate resistance at shallow depths, p_{cs}. By using this failure mode a smooth pile is assumed, and therefore no tangential forces occur at the pile surface. The active force is also computed from Rankine's failure mode, using the minimum coefficient of active earth pressure.

At deep depths the sand will, in contrast to shallow depths, flow around the pile and a statical failure mode as sketched in fig. 9 is used to calculate the ultimate resistance. The transition depth between these failure modes occurs, at the depth where the ultimate resistances calculated based on the two failure modes are identical.

The ultimate resistance per unit length of the pile can for the two failure modes be calculated according to (12) and (13):

$$p_{cs} = \gamma' x \frac{K_0 x \tan\varphi_{tr} \sin\beta}{\tan(\beta-\varphi_{tr})\cos\alpha} + \gamma' x \frac{\tan\beta}{\tan(\beta-\varphi_{tr})}(D - x\tan\beta\tan\alpha) + \gamma' x (K_0 x \tan\varphi_{tr}(\tan\varphi_{tr}\sin\beta - \tan\alpha) - K_a D) \quad (12)$$

$$p_{cd} = K_a D\gamma' x(\tan^8\beta - 1) + K_0 D\gamma' x \tan\varphi_{tr}\tan^4\beta \quad (13)$$

p_{cs} is valid for shallow depths and p_{cd} for deep depths, γ' is the effective unit weight, and φ_{tr} is the internal angle of friction based on triaxial tests. The factors α and β measured in degrees can be estimated by the following relations:

$$\alpha = \frac{\varphi_{tr}}{2} \quad (14)$$

$$\beta = 45° + \frac{\varphi_{tr}}{2} \quad (15)$$

Hence, the angle β is estimated according to Rankine's theory which is valid if the

pile surface is assumed smooth. The factor α depends on the friction angle and load type. However, the effect of load type is neglected in (14). K_a and K_0 are the coefficients of active horizontal earth pressure and horizontal earth pressure at rest, respectively:

$$K_a = \tan^2(45 - \frac{\varphi_{tr}}{2}) \tag{16}$$

$$K_0 = 0.4 \tag{17}$$

The value of K_0 depends on several factors, e.g. the friction angle, but (17) does not reflect that.

The theoretical ultimate resistance, p_c, as function of depth is shown in fig. 10. As shown, the transition depth increases with diameter and angle of internal friction. Hence, for piles with a low slenderness ratio the transition depth might appear far beneath the pile toe.

By comparing the theoretical ultimate resistance, p_c, with the full-scale tests at Mustang Island, Cox et al. (1974) found a poor agreement. Therefore, a coefficient A is introduced when calculating the actual ultimate resistance, p_u, employed in the p–y curve formulations:

$$p_u = Ap_c \tag{18}$$

The variation of the coefficient A with non-dimensional depth, x/D, is shown in fig. 11a. The deformation causing the ultimate resistance, y_u, cf. fig. 7, is defined as $3D/80$.

p–y curve formulation

The soil resistance per unit length, p_m, at $y_m = D/60$, cf. fig. 7, can be calculated as:

$$p_m = Bp_c \tag{19}$$

B is a coefficient depending on the non-dimensional depth x/D, as plotted in fig. 11b.

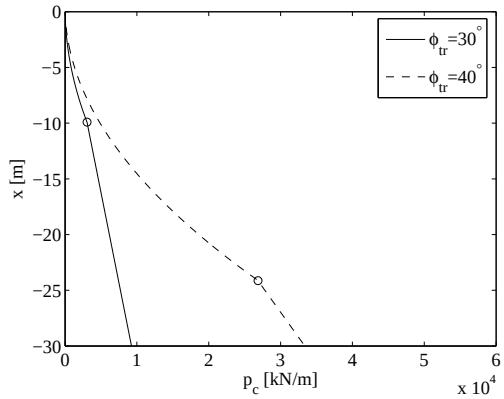

(a) $D = 1.0$ m

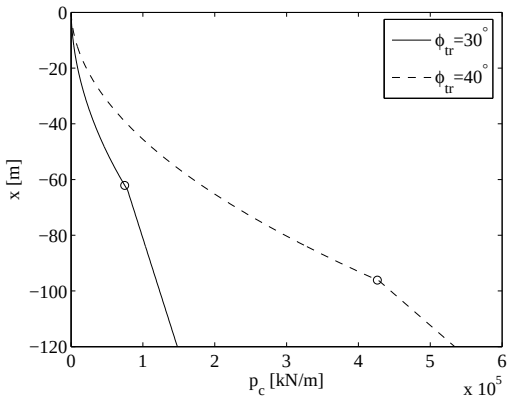

(b) $D = 4.0$ m

Figure 10: Theoretical ultimate resistance, p_c, as function of the depth. $\gamma' = 10$ kN/m^3 has been used to plot the figure. The transition depths are marked with circles.

The slope of the initial straight line, p_1 as shown in fig. 7, depends on the initial modulus of subgrade reaction, k, cf. tab. 1, and the depth x. This is due to the fact that the in-situ soil modulus of elasticity also increases with depth. Further, it is assumed that k increases linearly with depth since laboratory test shows, that the initial slope of the stress-strain curve for sand is a linear function of the confining pressure Terzaghi (1955). The initial straight line is given by:

$$p_1(y) = kxy \tag{20}$$

Reese et al. (1974) suggest that the value of k only depends on the relative density/internal friction angle for the sand. On basis of full-scale experiments values

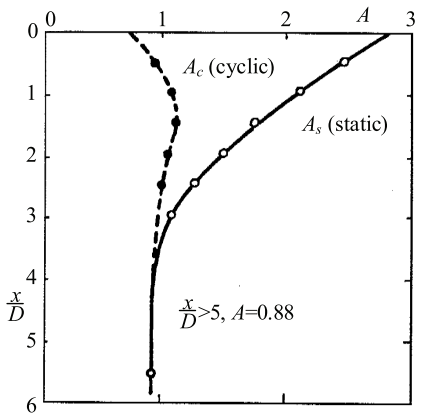

(a) Non-dimensional coefficient A for determining the ultimate soil response.

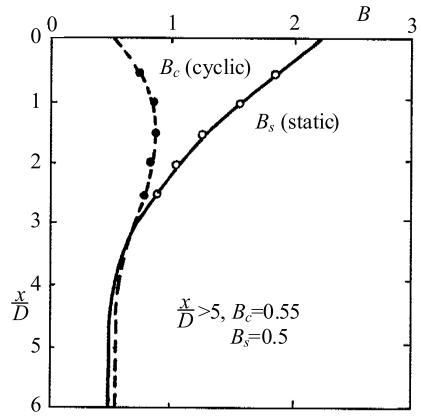

(b) Non-dimensional coefficient B for determining the soil response, p_m.

Figure 11: Non-dimensional variation of A and B, after Reese et al. (1974).

of k for loose sands, for medium sands, and for dense sands are 5.4 MN/m^3 (20 lbs/in^3), 16.3 MN/m^3 (60 lbs/in^3), and 34 MN/m^3 (125 lbs/in^3), respectively. The values are valid for sands below the water table. Earlier estimations of k has also been made, for example by Terzaghi (1955), but according to Reese and Van Impe (2001) these methods have been based on intuition and insight. Design regulations (e.g. API 1993 and DNV 1992) recommend the use of the curve shown in fig. 12. The curve only shows data for relative densities up to 80 %, which causes large uncertainties in the estimation of k for very dense sands.

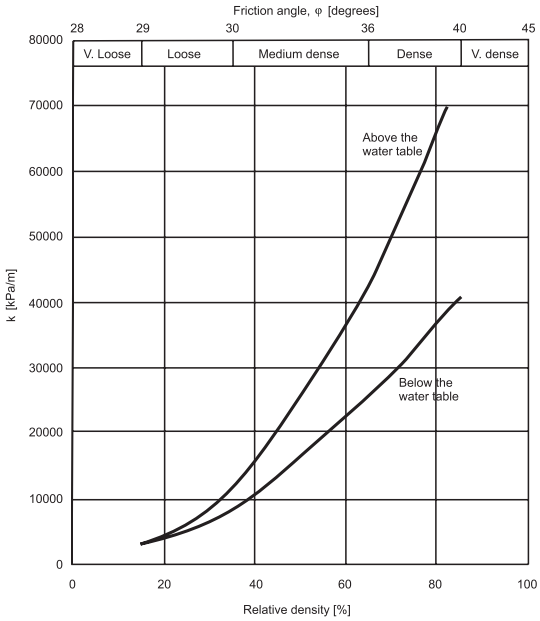

Figure 12: Variation of initial modulus of subgrade reaction k as function of relative density, after API (1993).

The equation for the parabola, p_2, cf. fig. 7, is described by:

$$p_2(y) = Cy^{1/n} \tag{21}$$

where C and n are constants. The constants and the parabola's start point (y_k,p_k) are determined by the following criteria:

$$p_1(y_k) = p_2(y_k) \tag{22}$$

$$p_2(y_m) = p_3(y_m) \tag{23}$$

$$\frac{\partial p_2(y_m)}{\partial y} = \frac{\partial p_3(y_m)}{\partial y} \tag{24}$$

The constants can then be estimated:

$$n = \frac{p_m}{my_m} \tag{25}$$

$$C = \frac{p_m}{y_m^{1/n}} \tag{26}$$

$$y_k = \left(\frac{C}{kx}\right)^{n/(n-1)} \tag{27}$$

where m is the slope of the line, p_3.

3.3 Method B

Design regulations (e.g. API 1993 and DNV 1992) suggest a modified formulation

of the p–y curves, in which the analytical expressions for the ultimate resistance, (12) and (13), are approximated using the dimensionless parameters C_1, C_2 and C_3:

$$p_u = \min \begin{pmatrix} p_{us} = (C_1 x + C_2 D)\gamma' x \\ p_{ud} = C_3 D \gamma' x \end{pmatrix} \tag{28}$$

The constants C_1, C_2 and C_3 can be determined from fig. 13.

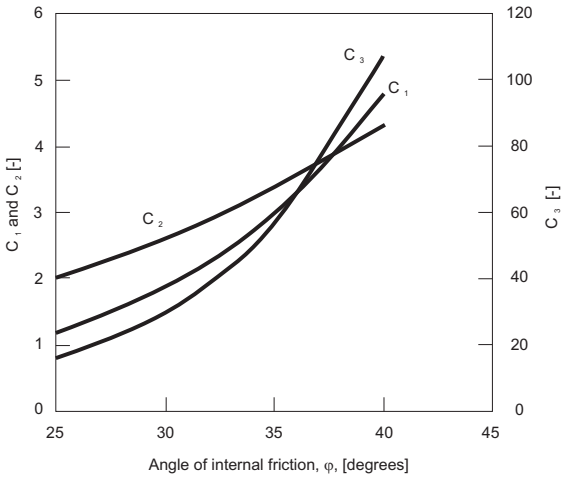

Figure 13: Variation of the parameters C_1, C_2 and C_3 as function of angle of internal friction, after API (1993).

A hyperbolic formula is used to describe the relationship between soil resistance and pile deflection instead of a piecewise formulation as proposed by method A:

$$p(y) = Ap_u \tanh(\frac{kx}{Ap_u} y) \tag{29}$$

The coefficient A could either be determined from fig. 11a or by:

$$A = \left(3.0 - 0.8\frac{H}{D}\right) \geq 0.9 \tag{30}$$

Since:

$$\frac{dp}{dy} \mid_{y=0} = Ap_u \frac{\frac{kx}{Ap_u}}{\cosh^2(\frac{kxy}{Ap_u})} \mid_{y=0} = kx \tag{31}$$

the p–y curve's initial slope is then similar using the two methods, cf. (20). Also the upper bound of soil resistance will approximately be the same. However, there is a considerable difference in soil resistance predicted by the two methods when considering the section between the points (y_k,p_k) and (y_u,p_u) as shown in fig. 14. The soil parameters from tab. 2 has been used to construct the p–y curves shown in fig. 14.

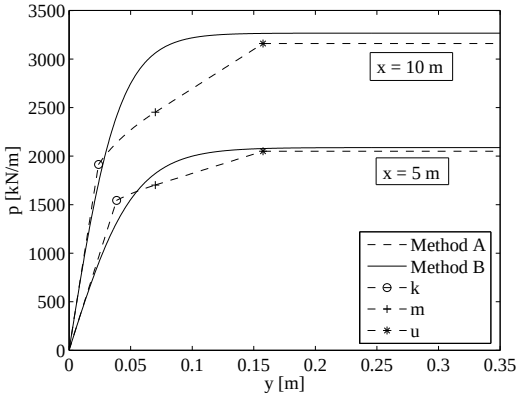

Figure 14: Example of p–y curves based on method A and B. The points k, m, and u refers to the points (y_k,p_k), (y_m,p_m), and (y_u,p_u), respectively, cf. fig. 7.

Table 2: Soil parameters used for plotting the p–y curves in fig. 14.

γ'	ϕ_{tr}	D	k
[kN/m^3]	[°]	[m]	[kN/m^3]
10	30	4.2	8000

3.4 Comparison of methods

A comparison of both static and cyclic p–y curves has been made by Murchison and O'Neill (1984) based on a database of 14 full-scale tests on 10 different sites. The pile diameters varied from 51 mm (2 in.) to 1.22 m (48 in.). Both timber, concrete and steel piles were considered. The soil friction angle ranged from 23° to 42°. The test piles' slenderness ratio's were not provided.

Murchison and O'Neill (1984) compared the different p–y curve formulations with the full-scale tests using the Winkler approach. The predicted head deflection, maximum moment, M_{max}, and the depth

of maximum moment were compared according to the error, E:

$$E = \frac{|\text{predicted value - measured value}|}{\text{measured value}} \tag{32}$$

In the analysis it was desired to assess the formulations ability to predict the behaviour of steel pipe monopiles. Multiplication factors were therefore employed. The error, E, was multiplied by a factor of two for pipe piles, 1.5 for non-pipe driven piles and a factor of one for drilled piers. When predicted values were lower than the measured values the error was multiplied by a factor of two. By using these factors unconservative results are penalised and pipe piles are valued higher in the comparison. In tab. 3 the average value of E for static p–y curves are shown for the two methods. As shown, method B results in a lower average value of E for all the criteria considered in the comparison. The standard deviation of E was not provided in the comparison.

Table 3: Average values of the error, E. The methods are compared for pile-head deflection, maximum moment and depth to maximum moment.

	Pile-head deflection	$M_{\max}$	Depth to $M_{\max}$
Method A	2.08	0.75	0.58
Method B	1.44	0.44	0.40

Murchison and O'Neill (1984) analysed the sensitivity to parameter variation for method B. The initial modulus of subgrade reaction, k, the internal friction angle, φ, and the effective unit weight, γ', were varied. They found that a 10 % increase in either φ or γ' resulted in an increase in pile-head deflection of up to 15 and 10 %, respectively. For an increase of 25 % in k an increase of up to 10 % of the pile-head deflection was found. The sensitivity analysis also shows that k has the greatest influence on pile-head deflection at small deflections and that φ has a great influence at large deflections. Murchison and O'Neill (1984) state that the sizes of the errors in tab. 3 can-not be explained by parameter uncertainty. The amount of data included in the database was very small due to the unavailability of appropriately documented full-scale tests and Murchison and O'Neill (1984) therefore concluded that a further study of the soil-pile interaction was needed.

4 Limitations of p–y curves

The p–y curve formulations for piles in cohesionless soils are, as described, developed for piles with diameters much less than 4 to 6 m which is often necessary for nowadays monopiles. Today, there is no approved method for dealing with these large diameter offshore piles, which is probably why the design regulations are still adopting the original p–y curves, cf. Reese et al. (1974), API(1993), and DNV(1992).

The p–y curve formulations are, as described, derived based on the Mustang Island tests which included only two piles and a total of seven load cases. Furthermore, the tests were conducted for only one pile diameter, one type of sand, only circular piles etc. Taken into account the number of factors that might affect the behaviour of a laterally loaded pile and the very limited number of full-scale tests performed to validate the method, the influence of a broad spectre of parameters on the p–y curves are still to be clarified. Especially when considering offshore wind turbine foundations a validation of stiff piles with a slenderness ratio of $L/D < 10$ is needed as the Mustang Island test piles had a slenderness ratio of $L/D = 34.4$. It is desirable to investigate this as it might have a significant effect on the initial stiffness which is not accounted for in the p–y curve method. Briaud et al. (1984) postulate that the soil response depends on the flexibility of the pile. Criteria for stiff ver-

sus flexible behaviour of piles have been proposed by various authors, for example Dobry et al. (1982), Budhu and Davies (1987), and Poulus and Hull (1989). The difference in deformation behaviour of a stiff and a flexible pile is shown in fig. 15. A pile behaves rigidly according to the following criterion, cf. Poulus and Hull (1989):

$$L < 1.48 \left(\frac{E_p I_p}{E_s} \right)^{0.25} \tag{33}$$

E_s is Young's modulus of elasticity of the soil. The criterion for a flexible pile behaviour is:

$$L > 4.44 \left(\frac{E_p I_p}{E_s} \right)^{0.25} \tag{34}$$

According to (33) a monopile with an outer diameter of 4 m, an embedded length of 20 m and a wall thickness of 0.05 m behaves rigidly if $E_s < 7.6$ MPa. In contrast, the pile exhibits a flexible behaviour if $E_s > 617$ MPa. Even dense sands have $E_s < 100$ MPa, so the recently installed monopiles behave, more like a rigid pile than a flexible.

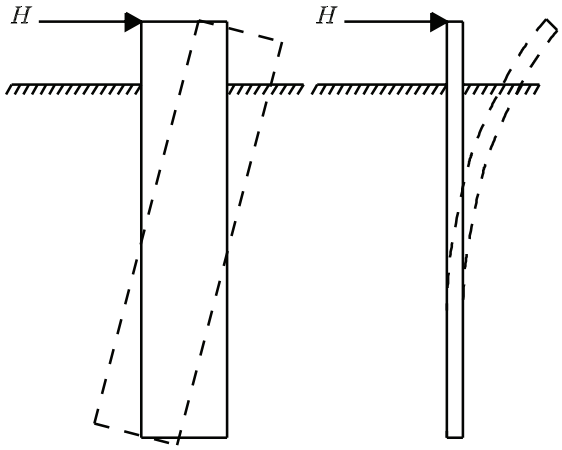

Figure 15: Rigid versus flexible pile behaviour.

For modern wind turbine foundations only small pile head rotations are acceptable. Furthermore, the strict demands to the total stiffness of the system due to resonance in the serviceability mode increase the significance of the p–y curve's initial slope and hereby the initial stiffness of the soil-pile system.

When using the p–y curve method the pile bending stiffness is employed when solving the beam on an elastic foundation problem. However, no importance is attached to the pile bending stiffness in the formulation of the p–y curves, hence E_{py} is independent of the pile properties. The validity of this assumption can be questioned as E_{py} is a parameter describing the soil-pile interaction.

When decoupling the non-linear springs associated with the Winkler approach another error is introduced since the soil in reality acts as a continuum.

In the following a number of assumptions and not clarified parameters related to the p–y curve method are treated separately. The treated assumptions and parameters are:

- Shearing force between soil layers.
- The ultimate soil resistance.
- The influence of vertical pile load on lateral soil response.
- Effect of soil-pile interaction.
- Diameter effect on initial stiffness of p–y curves.
- Choice of horizontal earth pressure coefficient.
- Shearing force at the pile toe.

4.1 Shearing force between soil layers

Employing the Winkler approach the soil response is divided into layers each represented by a non-linear spring. As the springs are uncoupled the layers are considered to be independent of the lateral

pile deflection above and below that specific layer, i.e. the soil layers are considered as smooth layers able to move relatively to each other without loss of energy to friction. Pasternak (1954) modified the Winkler approach by taking the shear stress between soil layers into account. The horizontal load per length of the pile is given by:

$$p(y) = -E_{py}^{p} y - G_s \frac{dy}{dx} \qquad (35)$$

where G_s is the soil shear modulus. The subgrade reaction modulus E_{py} given in tab. 1 may indirectly contain the soil shear stiffness as the p–y curve formulation is fitted to full-scale tests. E_{py}^{p} is a modulus of subgrade reaction without contribution from the soil shear stiffness.

Belkhir (1999) examines the significance of shear between soil layers by comparing the CAPELA design code, which takes the shear between soil layers into account, with the French PILATE design code, which deals with smooth boundaries. The two design codes are compared with the results of 59 centrifuge tests conducted on long and slender piles. Analyses show concordance between the two design codes when shear between soil layers is not taken into account. Furthermore, the analyses shows a reduction from 14 % to 5 % in the difference between the maximum moments determined from the centrifuge tests and the numerical simulations when taking the shear between the soil layers into account. However, it is not clear from the paper whether or not the shear between soil layers is dependent on pile diameter, slenderness ratio etc. Furthermore it is not clarified whether the authors distinguish between E_{py} and E_{py}^{p}.

4.2 The ultimate soil resistance

The p–y curve formulations according to Method A and Method B, cf. (12) and (29), are both dependent on the ultimate soil resistance. The method for estimating p_u is therefore evaluated in the following.

Failure modes

When designing large diameter monopiles in sand, the transition depth will most often occur beneath the pile toe, cf. fig. 10b. There are however several uncertainties concerning the ultimate resistance at shallow depths.

The prescribed method for calculating the ultimate resistance at shallow depths assumes that the pile is smooth, i.e. no skin friction appears and a Rankine failure mode will form. However, in reality a pile is neither perfectly rough nor perfectly smooth, and the assumed failure mechanism is therefore not exactly correct. According to Harremoës et al. (1984) a Rankine failure takes place for a perfectly smooth wall and a Prandtl failure for a perfectly rough wall, cf. fig. 16a and fig. 16b, respectively. Due to the fact that the pile is neither smooth nor rough a combination of a Rankine and Prandtl failure will occur. Furthermore, the failure modes are derived for a two-dimensional case.

In (12) the angle α, which determines the horizontal spread of the wedge, appears. Through experiments Reese et al. (1974) postulate that α depends on both the void ratio, friction angle, and the type of loading. However, the influence of void ratio and type of loading is neglected in the expression of α.

Nowadays monopiles are non-slender piles with high bending stiffness. The piles will therefore deflect as almost rigid piles and rather large deformations will occur beneath the point of zero deflection. However, when calculating the ultimate resistance according to method A and B the point of zero deflection is disregarded. For non-slender piles a failure mode as shown in fig. 17 could form. This failure mode

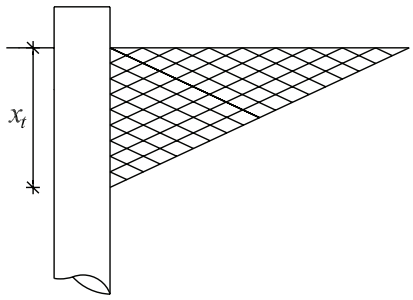

(a) Failure mode proposed by Rankine for a smooth surface at shallow depth.

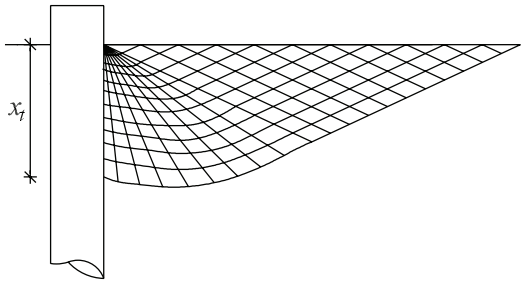

(b) Failure mode proposed by Prandtl for a rough surface at shallow depth.

Figure 16: Rankine and Prandtl failure modes.

is derived for a two-dimensional case and consists of stiff elastic zones and Rankine failures.

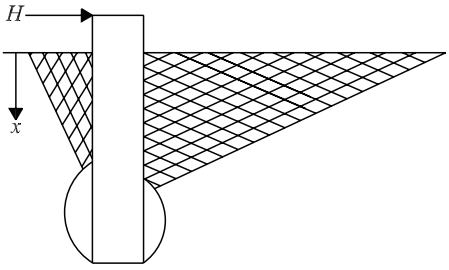

Figure 17: Failure mode for non-slender pile at shallow depth.

Soil dilatancy

The effect of soil dilatancy is not included in method A and B, and thereby the effects of volume changes during pile deflection are ignored.

Fan and Long (2005) investigated the influence of soil dilatancy on the ultimate resistance by use of a three-dimensional, non-linear finite element model. The constitutive model proposed by Desai et al. (1991) incorporating a non-associative flow rule was employed in the analyses. The finite element model was calibrated based on the full-scale tests at Mustang Island. The magnitudes of ultimate resistance were calculated for two compactions of one sandtype with similar friction angles but different angles of dilatancy. The dilatancy angles are not directly specified by Fan and Long (2005). Estimates have therefore been made by interpretation of the relation between volumetric strains and axial strains. Dilatancy angles of approximately 22° and 29° were found. An increase in ultimate resistance of approximately 50 % were found with the increase in dilatancy angle. In agreement with laboratory tests, where the dilatancy in dense sands contributes to strength, this makes good sense. However, as the dilatancy is increased and the friction angle is held constant extra strength is put into the material.

Alternative methods

Besides the prescribed method for calculating the ultimate resistance other formulations exist, see for example Broms (1964) and Hansen (1961). Fan and Long (2005) compared these methods with a finite element solution for various diameters, friction angles, and coefficients of horizontal earth pressure. Hansen's method showed the best correlation with the finite element model, whereas Broms' method resulted in conservative values of the ultimate resistance. Further, a significant difference between the finite element solution and the API method was found. The API method produces conservative results for shallow depths and unconservative results for deep depths. The results of the comparison are shown in fig. 18.

When calculating the ultimate soil resistance according to method A and B, the

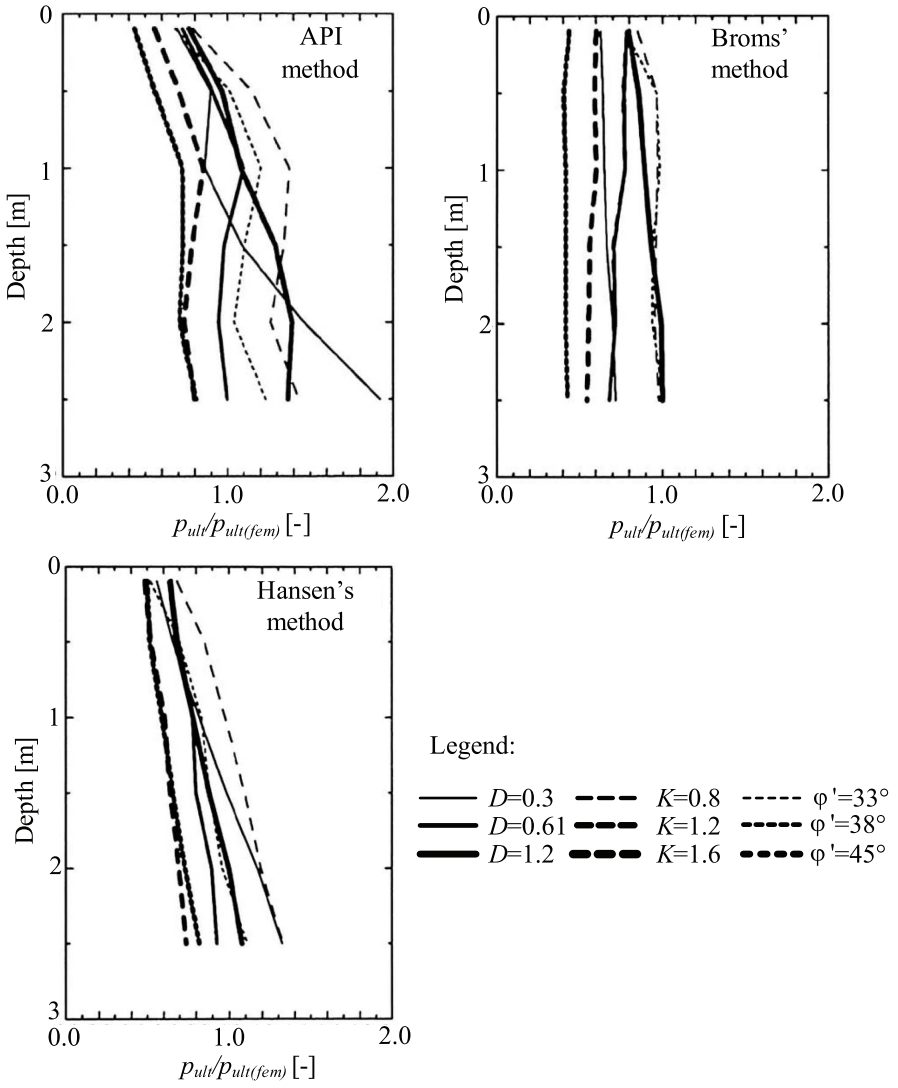

Figure 18: Comparison of the ultimate resistance estimated by Broms' method, Hansen's method and API's method with a finite element model, after Fan and Long (2005). $p_{ult}/p_{ult(fem)}$ defines the ratio of the ultimate resistance calculated by the analytical methods and the ultimate resistance calculated by the finite element model.

side friction as illustrated in fig. 19 is neglected. To take this into account Briaud and Smith (1984) has proposed a model where the ultimate resistance is calculated as the sum of the net ultimate frontal resistance and the net ultimate side friction. In the model both the net ultimate frontal resistance and the net ultimate side friction are taken to vary linearly with pile diameter. Zhang et al. (2005) refer to a comparison made by Barton and Finn (1983) of the model made by Briaud and Smith (1984) and lateral load tests performed in a centrifuge. The circular piles, associated with the tests, have diameters of 9, 12, and 16 mm and a slenderness ratio larger than 20. The magnitude of the acceleration in the centrifuge is not given. The ultimate resistance is compared for four depths and the error between measured and computed values is found to be less than 10 %. The methods proposed by Broms (1964) and Reese et al. (1974) are also compared with the model tests. Conclusions similar to Fan and Long (2005) are reached.

Side friction is due to the model proposed

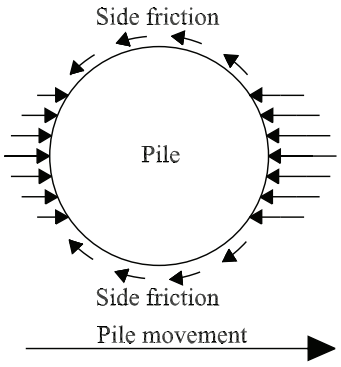

Figure 19: Side friction and soil pressure on the front and the back of the pile due to lateral deflection.

by Briaud and Smith (1984) unaffected by the diameter since both the ultimate frontal resistance and the net ultimate side friction vary linearly with diameter. However, the ultimate frontal resistance varies non-linearly with diameter in both the model proposed by Hansen (1961) and Reese et al. (1974). The importance of side friction might therefore be more significant for large diameter monopiles. Furthermore, it should be emphasized that the normal restistance at the back of the pile is neglected in the analysis.

Summary

Several assumptions are employed when calculating the ultimate resistance according to Reese et al. (1974) and the design regulations (e.g. API 1993 and DNV 1992). These methods do not account for friction between pile and soil as the pile surface is assumed smooth. Furthermore, the failure modes do not consider deflections beneath the point of zero deflection. Thus, the assumed failure modes might be inaccurate.

The dilatancy of the soil affects the soil response, but it is neglected in the p–y curve formulations.

Several methods for determining the ultimate resistance exist. The method proposed by Hansen (1961) were found to correlate better with a finite element model than the methods proposed by Reese et al. (1974) and Broms (1964). In order to take the effect of side friction into account a model was proposed by Briaud and Smith (1984). Predictions regarding the ultimate resistance correlate well with centrifuge tests.

4.3 The influence of vertical load on lateral soil response

In current practice, piles are analysed separately for vertical and horizontal behaviour. Karthigeyan et al. (2006) investigate the influence of vertical load on the lateral response in sand through a three-dimensional numerical model. In the model they adopt a Drucker-Prager constitutive model with a non-associated flow rule.

Karthigeyan et al. (2006) calibrate the numerical model against two different kinds of field data carried out by Karasev et al. (1977) and Comodromos (2003). Concrete piles with diameters of 0.6 m and a slenderness ratio of 5 were tested, cf. Karasev et al. (1977). The soil strata consisted of stiff sandy loam in the top 6 m underlain by sandy clay. Comodromos (2003) performed the tests in Greece. The soil profile consisted of silty clay near the surface with thin sublayers of loose sand. Beneath a medium stiff clay layer a very dense sandy gravel layer was encountered. Piles with a diameter of 1 m and a slenderness ratio of 52 were tested.

To investigate the influence of vertical load on the lateral response in sand Karthigeyan et al. (2006) made a model with a squared concrete pile (1200 $\times$ 1200 mm) with a length of 10 m. Two types of sand were tested, a loose and a dense sand with a friction angle of 30° and 36°, respectively. The vertical load was applied in two different ways, simultaneously with the lateral load, SAVL, and prior to the lateral load, VPL. Various values of verti-

cal load were applied. The conclusion of the analyses were that the lateral capacity of piles in sand increases under vertical load. The increase in lateral capacity depended on how the vertical load was applied as the highest increase was in the case of VPL. For the dense sand with a lateral deflection of 5 % of the side length the increase in lateral capacity was, in the case of SAVL, of up to 6.8 %. The same situation in the case of VPL resulted in an increase of up to 39.3 %. Furthermore, the analyses showed a large difference in the increase of lateral capacity between the two types of sand as the dense sand resulted in the highest increase. Due to vertical loads higher vertical soil stresses and thereby higher horizontal stresses occur, which also mobilise larger friction forces along the length of the pile. Therefore, the lateral capacity increases under the influence of vertical loading.

Although the analyses made by Karthigeyan et al. (2006) indicated a considerable increase in the lateral capacity at a relative high deflection, the improvement at small displacements are not as significant. Therefore it might not be of importance for wind turbine foundations.

4.4 Effect of soil-pile interaction

No importance is attached to the pile bending stiffness, E_pI_p, in the formulation of the p–y curves. Hereby, E_{py} is independent of the pile properties, which seems questionable as E_{py} is a soil-pile interaction parameter. Another approach to predict the response of a flexible pile under lateral loading is the strain wedge (SW) model developed by Norris (1986), which includes the pile properties. The concept of the SW model is that the traditional parameters in the one-dimensional Winkler approach can be characterised in terms of a three-dimensional soil-pile interaction behaviour.

The SW model parameters are related to a three-dimensional passive wedge developing in front of the pile subjected to lateral loading. The wedge has a form similar to the wedge associated with method A, as shown in fig. 8. However the angles α and β are given by:

$$\alpha = \varphi_m \tag{36}$$

$$\beta = 45° + \frac{\varphi_m}{2} \tag{37}$$

where φ_m is the angle of mobilised internal friction.

The purpose of the method is to relate the stresses and strains of the soil in the wedge to the subgrade reaction modulus, E_{py}. The SW model described by Ashour et al. (1998) assumes a linear deflection pattern of the pile over the passive wedge depth, h, as shown in fig. 20. The dimension of the passive wedge depends on two types of stability, local and global, respectively. To obtain local stability the SW model should satisfy equilibrium and compatibility between pile deflection, strains in the soil and soil resistance. This is obtained by an iterative procedure where an initial horizontal strain in the wedge is assumed.

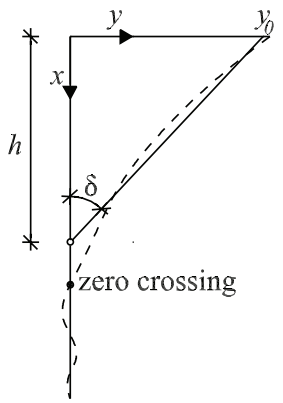

Figure 20: Linear deflection assumed in the SW-model, shown by the solid line. The dashed line shows the real deflection of a flexible pile. After Ashour et al. (1998).

After assuming a passive wedge depth the subgrade reaction modulus can be calculated along the pile. Based on the calculated subgrade reaction modulus the pile

head deflection can be calculated from the one-dimensional Winkler approach. Global stability is obtained when concordance between the pile head deflection calculated by the Winkler approach and the SW-model is achieved. The passive wedge depth is varied until global stability is obtained.

The pile bending stiffness influence the deflection calculated by the one-dimensional Winkler approach and hereby also the wedge depth. Hence, the pile bending stiffness influence the p–y curves calculated by the SW-model.

The equations associated with the SW model are based on the results of isotropic drained triaxial tests. Hereby an isotropic soil behaviour is assumed at the site. The SW model takes the real stresses into account by dealing with a stress level, defined as:

$$SL = \frac{\Delta\sigma_h}{\Delta\sigma_{hf}} \tag{38}$$

where $\Delta\sigma_h$ and $\Delta\sigma_{hf}$ are the mobilised horizontal stress change and the horizontal stress change at failure, respectively. The spread of the wedge is defined by the mobilised friction angle, cf. (36) and (37). Hence the dimensions of the wedge depends on the mobilised friction.

Although the SW model is based on the three-dimensional soil-pile interaction and it is dependent on both soil and pile properties there still are some points of criticism or doubt about the model. The model does not take the active soil pressure that occurs at the back of the pile into account. This seems to be a non-conservative consideration. Furthermore, the wedge only accounts for the passive soil pressure at the top front of the pile but neglects the passive soil pressure beneath the zero crossing point which will occur for a rigid pile, cf. section 4.2. The assumption of an isotropic behaviour of the soil in the wedge seems unrealistic in most cases for sand. To obtain isotropic behaviour the coefficient of horizontal earth pressure, K, needs to be 1, which is not the case for most sands. Effects of cyclic loading are not implemented in the SW model which is a large disadvantage seen in the light of the strict demands for the foundation design.

Ashour et al. (2002) criticise the p–y curve method as it is based and verified through a small number of tests. However the SW model, has according to Lesny et al. (2007) been verified only for conventional pile diameters.

Ashour et al. (2000) investigate by means of the SW model, the influence of pile stiffness on the lateral response for conditions similar to the Mustang Island tests. A p–y curve at a depth of 1.83 m is shown in fig. 21 for different values of E_pI_p. The p–y curve proposed by Reese et al. (1974) is also presented in the figure. It is seen that there is a good concordance between the experimental test and the SW model for similar pile properties. Furthermore, the soil resistance increases with increasing values of E_pI_p.

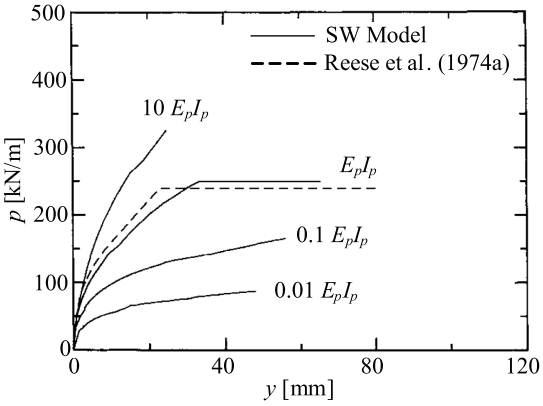

Figure 21: The influence of pile bending stiffness, after Ashour et al. (2000).

Changing the pile stiffness affects the p–y curves drastically according to the SW model. Fan and Long (2005) investigated the problem by changing the Young's modulus of elasticity of the pile while keeping the diameter and the second moment of inertia constant in their three-dimensional

finite element model. The results are shown in fig. 22. The investigation showed that the pile stiffness has neither significant influence on the ultimate bearing capacity nor the initial stiffness of the soil-pile system. The effect of pile stiffness shown in fig. 21 and 22 has not been verified trough experimental work.

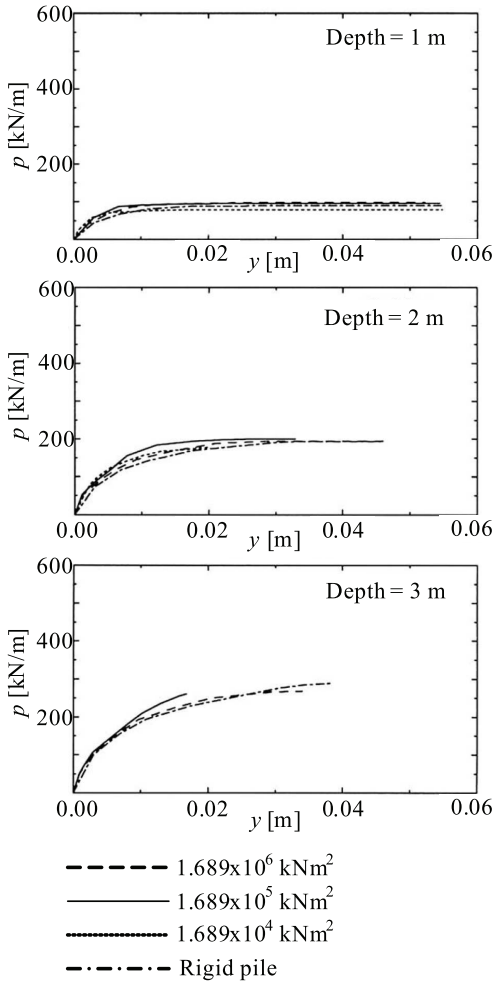

Figure 22: Effect of pile bending stiffness, after Fan and Long (2005).

4.5 Diameter effect on initial stiffness of p–y curves

The initial modulus of subgrade reaction, k, is according to API (1993), DNV (1992), and Reese et al. (1974) only dependent on the relative density of the soil as shown in fig. 12. Hence, the methods A and B do not include E_pI_p and D in the determination of k, which might seem surprisingly. Different studies on the consequences of neglecting the pile parameters have been conducted over time with contradictory conclusions. Ashford and Juirnarongrit (2003) point out the following three conclusions.

The first significant investigation was the analysis of stress bulbs conducted by Terzaghi (1955). Terzaghi concluded that by increasing the pile diameter the stress bulb formed in front of the pile is stretched deeper into the soil. This results in a greater deformation due to the same soil pressure at the pile. Terzaghi found that the soil pressure at the pile is linearly proportional to the inverse of the diameter giving that the modulus of subgrade reaction, E_{py} is independent on the diameter, cf. definitions in tab. 1.

Secondly, Vesic (1961) proposed a relation between the modulus of subgrade reaction used in the Winkler approach and the soil and pile properties. This relation showed that E_{py} is independent of the diameter for circular and squared piles.

Thirdly, Pender (1993) refers to two reports conducted by Carter (1984) and Ling (1988). Using a simple hyperbolic soil model they concluded that E_{py} is linear proportional to the pile diameter.

The conclusions made by Terzaghi (1955), Vesic (1961), and Pender (1993) concerns the subgrade reaction modulus, E_{py}. Their conclusions might also be applicable for the initial modulus of subgrade reaction, k, and the initial stiffness, E^*_{py}.

Based on the investigations presented by Terzaghi (1955), Vesic (1961), and Pender (1993), it must be concluded that no clear correlation between the initial modulus of subgrade reaction and the pile diameter has been realised. Ashford and Juirnarongrit (2005) contributed to the discussion with their extensive study of the problem which was divided into three

steps:

- Employing a simple finite element model.
- Analyses of vibration tests on large-scale concrete piles.
- Back-calculation of p–y curves from static load tests on the concrete piles.

The finite element analysis was very simple and did not account very well for the soil-pile interaction since friction along the pile, confining pressure in the sand, and gaps on the back of the pile were not included in the model. In order to isolate the effect of the diameter on the magnitude of E_{py}, the bending stiffness of the pile was kept constant when varying the diameter. The conclusion of the finite element analysis were that the diameter has some effect on the pile head deflection as well as the moment distribution. An increase in diameter leads to a decreasing pile head deflection and a decreasing depth to the point of maximum moment. However, it is concluded that the effect of increasing the diameter appears to be relatively small compared to the effect of increasing the bending stiffness, E_pI_p, which was not further investigated in the present case.

The second part of the work by Ashford and Juirnarongrit (2005) dealt with vibration tests on large-scale monopiles. The tests included three instrumented piles with diameters of 0.6, 0.9, and 1.2 m (12 m in length) and one pile with a diameter of 0.4 m and a length of 4.5 m. All piles were cast-in-drilled-hole and made up of reinforced concrete. They were installed at the same site consisting of slightly homogenous medium to very dense weakly cemented clayey to silty sand. The piles were instrumented with several types of gauges, i.e. accelerometers, strain gauges, tiltmeters, load cells, and linear potentiometers. The concept of the tests were that by subjecting the piles to small lateral vibrations the soil-pile interaction at small strains could be investigated by collecting data from the gauges.

Based on measured accelerations the natural frequencies of the soil-pile system were determined. These frequencies were in the following compared to the natural frequencies of the system determined by means of a numerical model. Two different expressions for the modulus of subgrade reaction, E_{py}, were used, one that is linearly dependent and one that is independent on the diameter. The strongest correlation was obtained between the measured frequencies and the frequencies computed by using the relation independent of the diameter. Hence, the vibration tests substantiate Terzaghi and Vesic's conclusions. It is noticed that the piles were only subjected to small deflections, hence $E_{py} \approx E^*_{py}$.

Finally, Ashford and Juirnarongrit (2005) performed a back-calculation of p–y curves from static load cases. From the back-calculation a soil resistance was found at the ground surface. This is in contraire to the p–y curves for sand given by Reese et al. (1974) and the recommendations in API (1993) and DNV (1992) in which the initial stiffness, E^*_{py}, at the ground surface is zero. The resistance at the ground surface might be a consequence of cohesion in the slightly cemented sand.

Furthermore, a comparison of the results from the back-calculations for the various pile diameters indicated that the effects of pile diameter on E^*_{py} were insignificant. The three types of analyses conducted by Ashford and Juirnarongrit (2005) indicate the same: the effect of the diameter on E^*_{py} is, insignificant.

Fan and Long (2005) investigated the influence of the pile diameter on the soil response by varying the diameter and keeping the bending stiffness, E_pI_p, constant in their finite element model. The results are given as curves normalised by the diameter and vertical effective stress as shown in

fig. 23. No significant correlation between diameter and initial stiffness is observed. It must be emphasised that the investigation considers only slender piles.

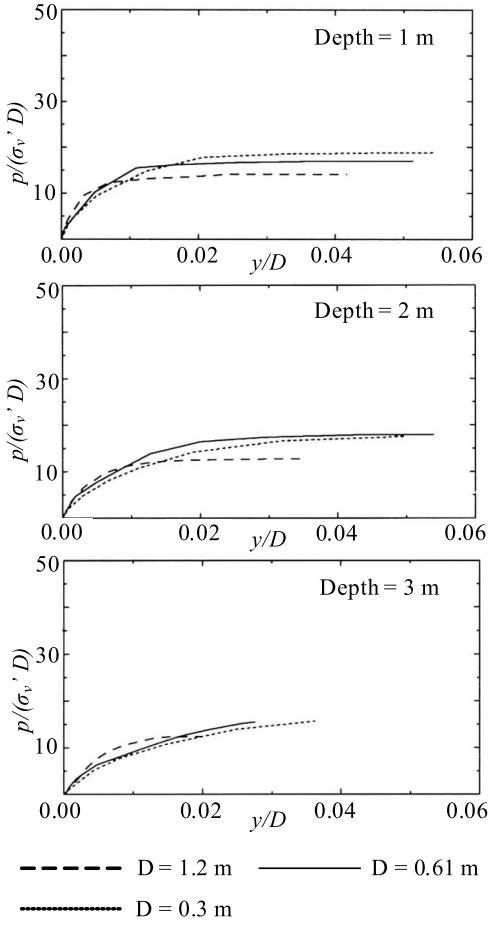

Figure 23: Effect of changing the diameter, after Fan and Long (2005).

For non-slender piles the bending stiffness might cause the pile to deflect almost as a rigid object. Therefore, the deflection at the pile toe might be significant. Thus a correct prediction of the initial stiffness is important in order to determine the correct pile deflection.

Based upon a design criterion demanding the pile to be fixed at the toe, Lesny and Wiemann (2006) investigated by back-calculation the validity of the assumption of a linearly increasing E^*_{py} with depth. The investigation indicated that E^*_{py} is overestimated for large diameter piles at great depths. Therefore, they suggested a parabolic relation, to be used instead of a linear relation, cf. fig. 24. A finite element model was made in order to validate the parabolic assumption. The investigations showed that employing the parabolic approach gave more similar deflections to the numerical modelling than by using the traditional linear approach in the p–y curve method. However, it was emphasised that the method should only be used for determination of pile length. The p–y curves still underestimates the pile head deflections even though the parabolic approach is used.

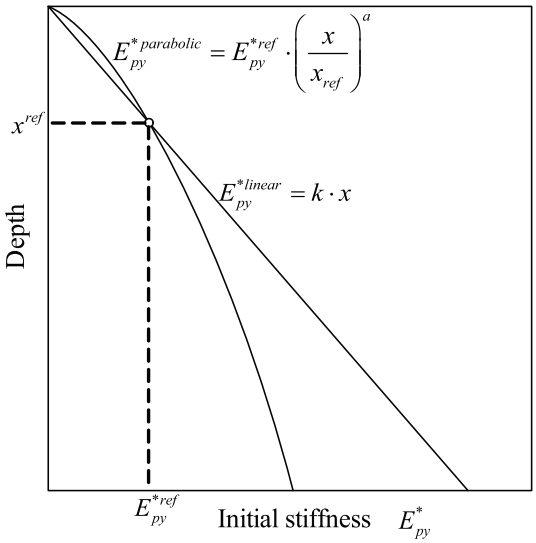

Figure 24: Variation of initial stiffness, E^*_{py}, as function of depth, after Lesny and Wiemann (2006). The linear approach is employed in Reese et al. (1974) and the design codes (e.g. API 1993, and DNV 1992). The exponent a can be set to 0.5 and 0.6 for dense and medium dense sands, respectively.

The above mentioned investigations are summarised in tab. 4. From this tabular it is obvious that more research is needed.

Looking at cohesion materials the tests are also few. According to Ashford and Juirnarongrit (2005) the most significant findings are presented by Reese et al. (1975), Stevens and Audibert (1979), O'Neill and Dunnavant (1984), and Dunnavant and O'Neill (1985).

Reese et al. (1975) back-calculated p–y

Table 4: Chronological list of investigations concerning the diameter effect on the initial stiffness of the p–y curve formulations.

Author	Method	Conclusion
Terzaghi (1955)	Analytical	Independent
Vesic (1961)	Analytical	Independent
Carter (1984)	Analytical expression calibrated against full-scale tests	Linearly dependent
Ling (1988)	Validation of the method proposed by Carter (1984)	Linearly dependent
Ashford and Juirnarongrit (2005)	Numerical and large-scale tests	Insignificant influence
Fan and Long (2005)	Numerical	Insignificant influence
Lesny and Wiemann (2006)	Numerical	Initial stiffness is non-linear for long and large diameter piles

curves for a 0.65 m diameter pile in order to predict the response of a 0.15 m pile. The calculations showed a good approximation of the moment distribution, but the deflections however were considerably underestimated compared to the measured values associated with the 0.15 m test pile.

Based on published lateral pile load tests Stevens and Audibert (1979) found that deflections computed by the method proposed by Matlock (1970) and API (1987) were overestimated. The overestimation increases with increasing diameter leading to the conclusion that an increase in modulus of subgrade reaction, E_{py}, occurs with an increase in diameter.

By testing laterally loaded piles with diameters of 0.27 m, 1.22 m, and 1.83 m in an overconsolidated clay, O'Neill and Dunnavant (1984) and Dunnavant and O'Neill (1985) found that there were a non-linear relation between deflection and diameter. They found that the deflection at 50 % of the ultimate soil resistance generally decreased with an increase in diameter. Hence, E_{py} increases with increasing pile diameter.

4.6 Choice of horizontal earth pressure coefficient

When calculating the ultimate resistance by method A the coefficient of horizontal earth pressure at rest, K_0, equals 0.4 even though it is well-known that the relative density/the internal friction angle influence the value of K_0. In addition, pile driving may increase the coefficient of horizontal earth pressure K.

The influence of the coefficient of horizontal earth pressure, K, are evaluated by Fan and Long (2005) for three values of K and an increase in ultimate resistance were found for increasing values of K. The increase in ultimate resistance is due to the fact, that the ultimate resistance is primarily provided by shear resistance in the sand, which depends on the horizontal stress.

Reese et al. (1974) and thereby API (1993) and DNV (1992) consider the initial modulus of subgrade reaction k to be independent of K. Fan and Long (2005) investigated this assumption. An increase in K results in an increase in confining pressure implying a higher stiffness. Hence, k is highly affected by a change in K and k increases with increasing values of K.

4.7 Shearing force at the pile toe

Recently installed monopiles have diameters around 4 to 6 m and a pile slenderness ratio around 5. Therefore, the bending stiffness, E_pI_p, is quite large compared to the pile length. The bending deformations of the pile will therefore be small and the pile will almost move as a rigid object as shown in fig. 25.

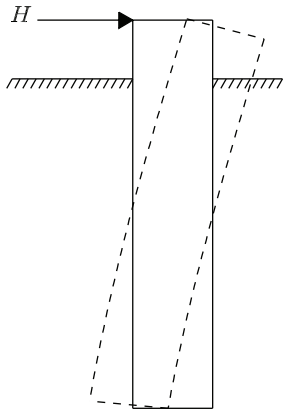

Figure 25: Deflection curve for non-slender pile.

As shown in fig. 25 there is a deflection at the pile toe. This deflection causes shearing stresses at the pile toe to occur, which increase the total lateral resistance. According to Reese and Van Impe (2001) a number of tests have been made in order to determine the shearing force at the pile toe, but currently no results from these tests have been published and no methods for calculating the shearing force as a function of the deflection have been proposed.

5 Conclusion

Monopiles are the most used foundation concept for offshore wind energy converters and they are usually designed by use of the p–y curve method. The p–y curve method is a versatile and practical design method. Furthermore, the method has a long history of approximately 50 years of experience.

The p–y curve method was originally developed to be used in the offshore oil and gas sector and has been verified with pile diameters up to approximately 2 m. Nowadays monopiles with diameters of 4 to 6 m and a slenderness ratio around 5 are not unusual.

In the present review a number of the assumptions and not clarified parameters associated with the p–y curve method have been described. The analyses considered in the review state various conclusions, some rather contradictory. However most of the analyses are based on numerical models and concentrates on piles with a slenderness ratio much higher than 5. In order to calibrate the p–y method to nowadays monopiles further numerical and experimental work is needed. Important findings of this paper are summarised as follows:

- When employing the Winkler approach the soil response is assumed independent of the deflections above and below any given point. The effect of involving the shear stress between soil layers seems to be rather small, and from the analysis it is not clear whether the results are dependent on pile properties.
- The failure modes assumed when dealing with the ultimate soil resistance at shallow depth seems rather unrealistic. In the employed methods the surface of the pile is assumed smooth. Furthermore, the method does not take the pile deflection into account, which seems critical for rigid piles.
- Soil dilatancy affects the soil response, but it is neglected in the p–y curve formulations.
- Determining the ultimate soil resistance by the method proposed by Hansen's (1961), seems to give more

reasonable results than the method associated with the design codes. Moreover, side friction is neglected in the design codes.

- In current practice piles are analysed separately for vertical and horizontal behaviour. Taking into account the effect of vertical load seems to increase the lateral soil resistance. However the effect is minor at small lateral deflections.

- Analyses of p–y curves sensitivity to pile bending stiffness, E_pI_p, gives rather contradictory conclusions. According to the Strain Wedge model the formulations of p–y curves are highly affected by pile bending stiffness. This is in contradiction to the existing p–y curves and a numerical analysis performed by Fan and Long (2005).

- The initial stiffness is independent of pile diameter according to the existing p–y curves. This agrees with analytical investigations by Terzaghi (1955), and Vesic (1961). Similarly, Ashford and Juirnarongrit (2005) concluded that initial stiffness is independent of the pile diameter based upon an analysis of a finite element model and tests on large scale concrete piles. Carter (1984) and Ling (1988) however, found that the initial stiffness is linear proportional to pile diameter. Based upon a numerical model, Lesny and Wiemann (2006) found that the initial stiffness is overpredicted at the bottom of the pile when considering large diameter piles.

- The initial stiffness of the p–y curve as well as the ultimate resistance increases with an increase in the coefficient of horizontal earth pressure. This effect is not taking into consideration in the existing p–y curve formulations.

- A pile which behaves rigidly will have a deflection at the pile toe. Taking this deflection into consideration might give an increase in net soil resistance.

6 References

Abdel-Rahman K., and Achmus M., 2005. Finite element modelling of horizontally loaded Monopile Foundations for Offshore Wind Energy Converters in Germany. *International Symposium on Frontiers in Offshore Geotechnics*, Perth, Australia, Sept. 2005. Balkerna.

API, 1993. Recommended practice for planning, designing, and constructing fixed offshore platforms - Working stress design, *API RP2A-WSD*, American Petrolium Institute, Washington, D.C., 21. edition.

Ashford S. A., and Juirnarongrit T., March 2003. Evaluation of Pile Diameter Effect on Initial Modulus of Subgrade Reaction. *Journal of Geotechnical and Geoenvironmental Engineering*, **129**(3), pp. 234-242.

Ashford S. A., and Juirnarongrit T., 2005. Effect of Pile Diameter on the Modulus of Subgrade Reaction. *Report No. SSRP-2001/22, Department of Structural Engineering, University of California, San Diego.*

Ashour M., Norris G., and Pilling P., April 1998. Lateral loading of a pile in layered soil using the strain wedge model. *Journal of Geotechnical and Geoenvironmental Engineering*, **124**(4), paper no. 16004, pp. 303-315.

Ashour M., and Norris G., May 2000. Modeling lateral soil-pile response based on soil-pile interaction. *Journal of Geotechnical and Geoenvironmental Engineering*, **126**(5), paper no. 19113, pp. 420-428.

Ashour M., Norris G., and Pilling P., August 2002. Strain wedge model capability of analyzing behavior of laterally loaded isolated piles, drilled shafts and pile groups. *Journal of Bridge Engineering*, **7**(4), pp. 245-254.

Banerjee P. K., and Davis T. G., 1978. The behavior of axially and laterally loaded single piles embedded in non-homogeneous soils. *Geotechnique*, **28**(3), pp. 309-326.

Barton Y. O., and Finn W. D. L., 1983. Lateral pile response and p–y curves from centrifuge tests. *Proceedings of the 15th Annual Offshore Technology Conference* , Houston, Texas, paper no. OTC 4502, pp. 503-508.

Belkhir S., Mezazigh S., and Levacher, D., December 1999. Non-Linear Behavior of Lateral-Loaded Pile Taking into Account the Shear Stress at the Sand. *Geotechnical Testing Journal*, GTJODJ, **22**(4), pp. 308-316.

Briaud J. L., Smith T. D., and Meyer, B. J., 1984. Using pressuremeter curve to design laterally loaded piles. *In Proceedings of the 15th Annual Offshore Technology Conference*, Houston, Texas, paper no. OTC 4501.

Broms B. B., 1964. Lateral resistance of piles in cohesionless soils. *Journal of Soil Mechanics and Foundation Div.*, **90**(3), pp. 123-156.

Budhu M., and Davies T., 1987. Nonlinear Analysis of Laterally loaded piles in cohesionless Soils. *Canadian geotechnical journal*, **24**(2), pp. 289-296.

Carter D. P., 1984. A Non-Linear Soil Model for Predicting Lateral Pile Response. *Rep. No. 359, Civil Engineering Dept,. Univ. of Auckland, New Zealand.*

Comodromos E. M., 2003. Response prediction for horizontally loaded pile groups. *Journal of the Southeast Asian Geotechnical Society*, **34**(2), pp. 123-133.

Cox W. R., Reese L. C., and Grubbs B. R., 1974. Field Testing of Laterally Loaded Piles in Sand. *Proceedings of the Sixth Annual Offshore Technology Conference*, Houston, Texas, paper no. OTC 2079.

Desai C. S., Sharma K. G., Wathugala G. W., and Rigby D. B., 1991. Implementation of hierarchical single surface δ_0 and δ_1 models in finite element procedure. *International Journal for Numerical & Analytical Methods in Geomechanics*, **15**(9), pp. 649-680.

DNV, 1992. Foundations - Classification Notes No 30.4, Det Norske Veritas, Det Norske Veritas Classification A/S.

Dobry R., Vincente E., O'Rourke M., and Roesset J., 1982. Stiffness and Damping of Single Piles. *Journal of geotechnical engineering*, **108**(3), pp. 439-458.

Dunnavant T. W., and O'Neill M. W., 1985. Performance analysis and interpretation of a lateral load test of a 72-inch-diameter bored pile in overconsolidated clay. *Report UHCE 85-4*, Dept. of Civil Engineering., University of Houston, Texas, p. 57.

Fan C. C., and Long J. H., 2005. Assessment of existing methods for predicting soil response of laterally loaded piles in sand. *Computers and Geotechnics* **32**, pp. 274-289.

Hansen B. J., 1961. *The ultimate resistance of rigid piles against transversal forces.* Danish Geotechnical Institute, Bull. No. 12, Copenhagen, Denmark, 5-9.

Harremoës P., Ovesen N. K., and Jacobsen H. M., 1984. *Lærebog i geoteknik 2*, 4. edition, 7. printing. Polyteknisk Forlag, Lyngby, Danmark.

Hetenyi M., 1946. *Beams on Elastic Foundation.* Ann Arbor: The University of Michigan Press.

Karasev O. V., Talanov G. P., and Benda S. F., 1977. Investigation of the work of single situ-cast piles under different load combinations. *Journal of Soil Mechanics and Foundation Engineering*, translated from Russian, **14**(3), pp. 173-177.

Karthigeyan S., Ramakrishna V. V. G. S. T., and Rajagopal K., May 2006. Influence of vertical load on the lateral response of piles in sand. *Computers and Geotechnics* **33**, pp. 121-131.

LeBlanc C., Houlsby G. T., and Byrne B. W., 2007. Response of Stiff Piles to Long-term Cyclic Loading.

Lesny K., and Wiemann J., 2006. Finite-Element-Modelling of Large Diameter Monopiles for Offshore Wind Energy Converters. *Geo Congress 2006, February 26 to March 1*, Atlanta, GA, USA.

Lesny K., Paikowsky S. G., and Gurbuz A., 2007. Scale effects in lateral load response of large diameter monopiles. *Geo-Denver 2007 February 18 to 21*, Denver, USA.

Ling L. F., 1988. Back Analysis of Lateral Load Test on Piles. *Rep. No. 460, Civil Engineering Dept., Univ. of Auckland, New Zealand.*

Matlock H., and Reese L. C., 1960. Generalized Solutions for Laterally Loaded Piles. *Journal of the Soil Mechanics and Foundations Division*, **86**(5), pp. 63-91.

Matlock H., 1970. Correlations for Design of Laterally Loaded Piles in Soft Clay. *Proceedings, Second Annual Offshore Technology Conference*, Houston, Texas, paper no. OTC 1204, pp. 577-594.

McClelland B., and Focht J. A. Jr., 1958. Soil Modulus for Laterally Loaded Piles. *Transactions.* ASCE 123: pp. 1049-1086.

Murchison J. M., and O'Neill M. W, 1984. Evaluation of *p–y* relationships in cohesionless soils. *Analysis and Design of Pile Foundations. Proceedings of a Symposium in conjunction with the ASCE National Convention*, pp. 174-191.

Norris G. M., 1986. Theoretically based BEF laterally loaded pile analysis. *Proceedings, Third Int. Conf. on Numerical Methods in offshore piling*, Editions Technip, Paris, France, pp. 361-386.

O'Neill M. W., and Dunnavant T. W., 1984. A study of effect of scale, velocity, and cyclic degradability on laterally loaded single piles in overconsolidated clay. *Report UHCE 84-7*, Dept. of Civ. Engrg., University of Houston, Texas, p. 368.

Pasternak P. L., 1954. On a New Method of Analysis of an Elastic Foundation by Means of Two Foundation Constants, *Gosudarstvennoe Izadatelstro Liberatuni po Stroitelstvui Arkhitekture*, Moskow, pp. 355-421.

Peck R. B., Hanson W. E., and Thornburn T. H., 1953. *Foundation Engineering*, John Wiley and Sons, Inc. New York.

Pender M. J., 1993. Aseismic Pile Foundation Design Analysis. *Bull. NZ Nat. Soc. Earthquake Engineering.*, **26**(1), pp. 49-160.

Poulos H. G., 1971. Behavior of laterally loaded piles: I - Single piles. *Journal of the Soil Mechanics and Foundations Division*, **97**(5), pp. 711-731.

Poulos H. G., and Davis E. H., 1980. *Pile foundation analysis and design*, John Wiley & Sons.

Poulus H., and Hull T., 1989. The Role of Analytical Geomechanics in Foundation Engineering. *in Foundation Eng.: Current principles and Practices*, **2**, pp. 1578-1606.

Reese L. C., and Matlock H., 1956. Non-dimensional Solutions for Laterally Loaded Piles with Soil Modulus Assumed Proportional to Depth. *Proceedings of the*

eighth Texas conference on soil mechanics and foundation engineering. Special publication no. 29.

Reese L. C., Cox W. R., and Koop, F. D., 1974. Analysis of Laterally Loaded Piles in Sand. *Proceedings of the Sixth Annual Offshore Technology Conference*, Houston, Texas, **2**, paper no. OTC 2080.

Reese L. C., and Welch R. C., 1975. Lateral loading of deep foundation in stiff clay. *Journal of Geotechnic Engineering.*, Div., **101**(7), pp. 633-649.

Reese L. C., and Van Impe W. F., 2001. *Single Piles and Pile Groups Under Lateral Loading*, Taylor & Francis Group plc, London.

Stevens J. B., and Audibert J. M. E., 1979. Re-examination of p-y curve formulation. *Proceedings Of the XI Annual Offshore Technology Conference*, Houston, Texas, OTC 3402, pp. 397-403.

Terzaghi K., 1955. Evaluation of coefficients of subgrade reaction. *Geotechnique*, **5**(4), pp. 297-326.

Timoshenko S. P., 1941. Strength of materials, part II, advanced theory and problems, 2nd edition, 10th printing. New York: D. Van Nostrand.

United Nations, 1998. Kyoto protocol. *United Nations framework convention on climate change.*

Vesic A. S., 1961. Beam on Elastic Subgrade and the Winkler's Hypothesis. *Proceedings of the 5th International Conference on Soil Mechanics and Foundation Engineering*, Paris, **1**, pp. 845-850.

Winkler E., 1867. Die lehre von elasticzitat and festigkeit (on elasticity and fixity), Prague, 182 p.

Zhang L., Silva F., and Grismala R., January 2005. Ultimate Lateral Resistance to Piles in Cohesionless Soils. *Journal of Geotechnical and Geoenvironmental Engineering*, **131**(1), pp. 78-83.

ISSN 1901-726X
DCE Technical Report No. 57